ChemComm

A visible light-controllable Rho kinase inhibitor based on a photochromic phenylazothiazole

Journal:	*ChemComm*
Manuscript ID	CC-COM-09-2021-004905.R1
Article Type:	Communication

COMMUNICATION

A visible light-controllable Rho kinase inhibitor based on a photochromic phenylazothiazole

Received 00th January 20xx,
Accepted 00th January 20xx

DOI: 10.1039/x0xx00000x

Kazuya Matsuo,*[†a] Sampreeth Thayyil,[a] Mitsuyasu Kawaguchi,[b] Hidehiko Nakagawa[b] and Nobuyuki Tamaoki*[a]

Rho-associated coiled-coil-containing protein kinase (ROCK) is a serine-threonine kinase, whose inhibitors are useful for the regulation of actomyosin system. Here, we developed a photoswitchable ROCK inhibitor based on a phenylazothiazole scaffold. The reversible *trans-cis* isomerization by visible light stimuli enabled us to manipulate ROCK activities *in vitro* and in cells.

Rho-associated coiled-coil containing protein kinase (ROCK) is a 160 kDa serine-threonine kinase, which can be activated upon binding of RhoA-GTP to exhibit diverse biofunctions, especially those related to the cytoskeletal formation, cytokinesis, cell apoptosis, morphology, migration, and invasion.[1] ROCK mainly targets the phosphorylation of the actomyosin system, including myosin light chain II (MLC-2) and myosin phosphatase.[2]

To date, numerous small molecule inhibitors targeting ROCK have been elaborately developed by medicinal chemists to specifically deactivate the Rho-ROCK-based cellular signaling.[3] A few ROCK inhibitors have also been used clinically for treating cerebral vasospasm, and glaucoma. However, since there exists no strategy to control the activity of these inhibitors via the external stimuli, *in situ* regulation of ROCK remains challenging. As the pioneering research on the external stimulus-responsive ROCK inhibitors, N. M. Nascone-Yoder *et al.* reported the photocaged ROCK inhibitor "caged Rockout" (Figure 1a), which is composed of the ROCK inhibitor moiety masked with the photolabile protective group, 6-nitropiperonyloxymethyl.[4] Caged Rockout exhibits no inhibition of ROCK activity in the absence of light illumination, whereas it releases the ROCK inhibitor concomitantly with the ultraviolet light (365 nm) illumination, showing ROCK inhibition with high spatiotemporal resolution. Using this irreversible photocaging strategy, the function of ROCK in left-right asymmetric morphogenesis in *Xenopus laevis* embryos has been revealed successfully. Certainly, this work demonstrates the significant advances in a photoresponsive ROCK inhibitor, but there still exist some inherent drawbacks in the use of photocaging strategy. Ultraviolet light illumination is generally necessary for uncaging reactions, which is intrinsically harmful to biological components. Moreover, as the caging approach offers just a one-way photocontrol, it is only possible to switch the protein bioactivity from ON to OFF or *vice versa*, and is not a reversible mode. The reversible photoswitching of ROCK activities can contribute to the asymmetric regulation of actomyosin system including cytokinesis and cell migration with high spatiotemporal resolution, but there is no report about the reversibly controllable ROCK inhibitors to date.

Alternatively, the reversibly photocontrollable chemical tools including photostatins and optojasps have been intriguingly developed in recent years.[5] Photochromic moieties, as represented by azobenzenes, spiropyrans, diarylethenes, and so on, are elaborately incorporated into the pharmacophores of targeted biomolecules.[6] Recently, we also reported photoswitchable substrates and inhibitors of motor proteins on the basis of *trans-cis* photoisomerization of azobenzene derivatives.[7] However, with a few exceptions,[8] most reversible photoswitches need to exert ultraviolet light for at least one way of photoconversions. Using these photochromic moieties, several photoswitchable kinase ligands have been developed[9], but it often suffers from the small activity differences between thermodynamically stable isomers and metastable isomers, which can prevent the further cellular applications.

Herein, we describe the development of a reversibly photocontrollable ROCK inhibitor containing a phenylazothiazole scaffold as a reversible photoswitch with visible light stimuli for both the ways of photoconversion. *In vitro* kinase assay revealed that our photochemical tool can

[a] *Research Institute for Electronic Science, Hokkaido University, Kita 20, Nishi 10, Kita-ku, Sapporo, 001-0020, Japan. E-mail: tamaoki@es.hokudai.ac.jp for N.T.*
[b] *Graduate School of Pharmaceutical Sciences, Nagoya City University, 3-1, Tanabedori, Mizuho-ku, Nagoya, 467-8603, Japan.*
[†] *Present address: Faculty of Molecular Chemistry and Engineering, Kyoto Institute of Technology, Matsugasaki, Sakyo-ku, Kyoto, 606-8585, Japan. E-mail: kmatsuo@kit.ac.jp*

Electronic Supplementary Information (ESI) available: Experimental procedures, compound characterization, photoisomerization, thermal stability of *cis* isomer of **2**, *in vitro* kinase assay, immunofluorescence experiments, live cell experiments See DOI: 10.1039/x0xx00000x

regulate the ROCK activity with approximately 10-fold change between *trans*- and *cis*-rich states. Furthermore, its applicability to cells was verified through a biochemical analysis of the ROCK-dependent phosphorylation and the fluorescence imaging of actin stress fibers.

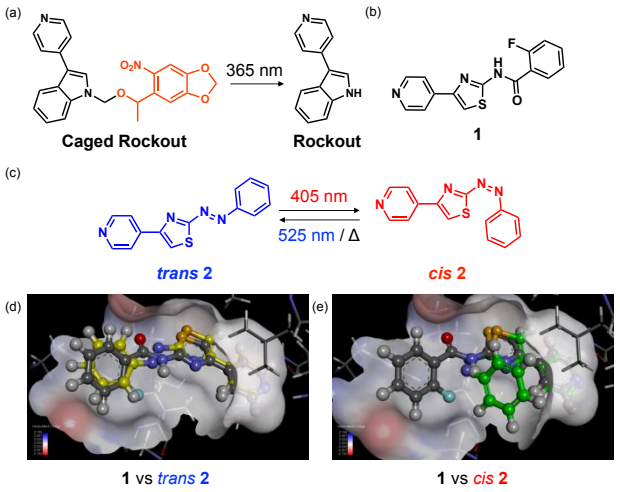

Figure 1. Rho-associated coiled-coil containing protein kinase (ROCK) inhibitors. (a) Uncaging reaction of photocaged ROCK inhibitor[4]. (b) The standard ROCK inhibitor **1**[10]. (c) Structure and photoisomerization of photoswitchable ROCK inhibitor **2** developed in the present study. (d) *trans* **2** (yellow-coloured carbon) superimposed with non-photoresponsive ROCK inhibitor **1** (grey-coloured carbon) in ROCK1 (PDB : 4YVC), which was simulated using a DiscoveryStudio software (e) The same as (d) except with *cis* **2** (green-coloured carbon).

To design the photocontrollable ROCK inhibitor, we first analyzed the X-ray co-crystal structure (PDB ID: 4YVC) of ROCK1, one of the isozymes of ROCK 1 and 2,[2] bound with the thiazole type of inhibitor **1**, which has been identified through the high-throughput screening[10] (Figure 1b, Figure S1). In detail, the pyridine ring of **1** formed the hydrogen bond with Met156 in ROCK. The carbonyl group in the amide of **1** could interact with the catalytic Lys105 residue. The benzene ring in **1** could slightly interact with the hydrophobic surface composed of Phe87 in ROCK. These interactions inspired us to replace the amide group with an azo group (-N=N-) through the strategy of 'azologization' coined by Trauner[11]. In addition, the fluorine group on the benzene ring was removed for the simplified design and synthesis, although the *ortho*-fluorine substituted azobenzene was reported to display the interesting photochemical properties including the significant enhancement of thermal stability of *cis* isomer[12]. Thus, we designed **2** as a candidate of a photoswitchable ROCK inhibitor (Figure 1c-d).

We synthesized the phenylazothiazole derivative **2** by the reaction of 4-(2-bromoacetyl)pyridine with the corresponding thiosemicarbazide in the presence of triethylamine and triphenylphosphine through the formation of the thiazole ring and azo group (Scheme S1),[13] which was characterized by ^{1}H-NMR, ^{13}C-NMR and HR-MS (Figures S3 and S4).

The photophysical properties of **2** (20 μM) in an aqueous solution were determined by UV-Vis absorption spectroscopy (Figure 2a). The absorption spectrum of **2** (100% *trans* isomer) without light illumination exhibited π-π* (near 385 nm) and n-π* (near 475 nm) transition bands, which was red-shifted with about 50 nm compared with the parent azobenzene. It was drastically altered upon light illumination at 405 nm to reach a photostationary state (PSS_{405nm}), where the *cis* isomer was predominantly formed (94% of *cis* isomer composition) as revealed by high performance liquid chromatography (HPLC) analysis (Figure S5) and nuclear magnetic resonance (NMR) analysis (Figure S6). The PSS_{525nm} with light illumination at 525 nm exhibited a *trans*-rich spectrum with 77-83% *trans* isomer composition. These photo-induced alterations in the absorption spectra were repeatedly performed without exhaustion (Figure 2b). In addition, the thermal stability of *cis*-**2** in an aqueous solution at 37 ºC was found to be 32 min (lifetime τ of the *cis* isomer) (Figure S7).

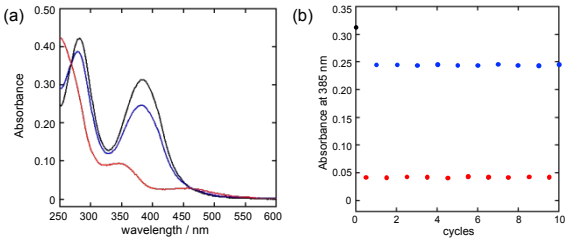

Figure 2. Photophysical properties of photoswitchable ROCK inhibitor **2**. (a) Absorption spectra of **2** (20 μM) in aqueous solution (acetonitrile : BRB80 buffer = 1 : 1) with or without light illumination at 405 nm (100 mW/cm², for 20 sec) and 525 nm (100 mW/cm², for 30 sec) at 25 ºC. Black line : before light illumination. Red line : Photostationary state for 405 nm. Blue line : Photostationary state for 525 nm. (b) Repetition of photoisomerization of **2** for 10 cycles. Black circle : before light illumination. Red circle : Photostationary state for 405 nm. Blue circle : Photostationary state for 525 nm.

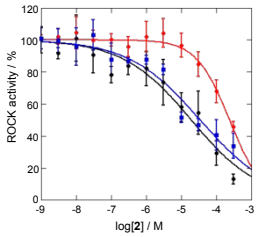

Figure 3. *In vitro* kinase assay results using photoswitchable ROCK inhibitor **2** with or without light illumination at 405 nm (100 mW/cm², 10 sec, every 5 min) and 525 nm (100 mW/cm², 10 sec, every 5 min) at 25 ºC. Black circle : **2** without light illumination. Blue square : **2** with 525 nm light illumination. Red circle : **2** with 405 nm light illumination. Error bars show the standard errors from triplicate experiments.

A similar photoswitch based on 4,5-disubstituted phenylazothiazole was recently explored for a photoswitchable inhibitor of p38α mitogen-activated protein kinase and the highly related casein kinase 1δ, which exhibited a *trans-cis* photoconversion of estimated more than 80% in UV-Vis spectra using light illumination at 435 nm and 525 nm.[9c] However, the 4,5-disubstituted phenylazothiazole derivative was reported to undergo the reduction of the azo group (-N=N-) in the presence of reductants including dithiothreitol (DTT) and glutathione (GSH) to form the corresponding hydrazine (-NH-NH-) derivative, which can misestimate the actual potencies of each isomers. To address this possibility, we also verified the stability towards DTT and GSH of **2** based on the photoswitch of 4-monosubstituted phenylazothiazole. As a result, **2** exhibited negligible response to 0.1 mM DTT used in the following *in vitro* kinase assay and 1.0 mM GSH of an intracellular antioxidant for 1 h with and without light

illumination at 405 nm (Figure S8). Hence, these photophysical properties controllable with visible light stimulus highlight our photoswitch of 4-monosubstituted phenylazothiazole developed in this study, which can accelerate the further biological applications, when compared to the irreversible photocaging strategy and the reversible photoswitch strategy using harmful ultraviolet light stimulus.

Next, we evaluated the inhibitory effects of **2** through an *in vitro* kinase assay with purified ROCK1 using the chemiluminescent ADP-Glo system (Promega, Madison, WI, USA) (Figure 3). The *trans* rich states of **2** without light illumination (100% *trans* isomer) and at $PSS_{525\ nm}$ exhibited the potent inhibitory activity (IC_{50} = 19 ± 5.5 μM before illumination and IC_{50} = 34 ± 9.3 μM at $PSS_{525\ nm}$), which was comparable to that of non-photoresponsive ROCK inhibitor **1** (IC_{50} = 8.2 ± 1.8 μM, Figure S9). In contrast, *cis* rich state of **2** at $PSS_{405\ nm}$ exhibited lesser potent inhibition activity (IC_{50} = 238 ± 26 μM at $PSS_{405\ nm}$) than *trans*-rich states of **2**. Although the affinity towards ROCK2 was not explored in this study, **2** is a promising photoswitchable ROCK1 inhibitor with approximately 10-fold affinity change between *trans* and *cis* states in test tubes. These results suggest that **2** can function at a certain range of concentration as a ROCK inhibitor before illumination or after light illumination at 525 nm and a non-ROCK inhibitor after light illumination at 405 nm.

The feasibility of **2** in cell-based experiments as a photoswitchable ROCK inhibitor was studied. ROCK catalyzes the phosphorylation of MLC-2 to mediate various cellular processes such as muscle contraction, cell motility and cytokinesis. Thus, the MLC-2 phosphorylation in Balb3T3 cells was analyzed through western blot analyses using antibodies against MLC-2 and phosphorylated MLC-2.[14] Figure 4 shows that the intensities of bands corresponding to the phosphorylated MLC-2 with *trans*-rich states of **2** without light illumination (lane 2) and under 525 nm light illumination (lane 4) are comparable to that of standard ROCK inhibitor **1** (lane 5). In contrast, the band intensity for the *cis*-rich state under 405 nm light illumination was almost the same as that noted for the dimethyl sulfoxide (DMSO) control (lane 3 vs. 1). Therefore, our biochemical analyses confirmed that **2** functioned as a photoswtichable ROCK inhibitor based on the *trans-cis* isomerization of the azo-group evoked by visible light illumination at two different wavelengths in cells.

ROCK is also a key modulator of actin stress fibers, which are the contractile bundles of actomyosin facilitating cell adhesion, migration, etc.[14] Therefore, we demonstrated the photocontrol of ROCK-dependent organization of actin stress fibers using **2**. After induction of stress fibers by serum starvation of Balb3T3 cells overnight, cells were incubated with **2** (100 μM) for 1h. The starved cells were subjected to the visualization of stress fibers using the rhodamine-phalloidin. Under no or 525 nm light illumination, cells with the *trans*-rich states of **2** exhibited no fiber-like structure, which indicated an obvious disorganization of actin stress fibers (Figure 5). This phenotype was also found in non-photoresponsive ROCK inhibitor **1**-treated cells (Figure S8). In contrast, the *cis*-rich state of **2** under the exposure to 405 nm light preserved the stress fiber organization similar to that with DMSO treatment (Figure S10). Therefore, it was suggested that **2**, with cell permeability, reversibly led to the disorganization of actin stress fibers depending on the ROCK activity in cells.

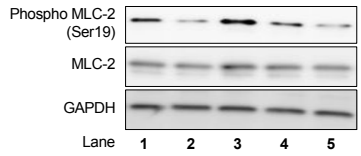

Figure 4. Western blot analysis of target protein expression for evaluation of intracellular ROCK activity in the presence of **2** (100 μM) with light stimuli. GAPDH (Glyceraldehyde-3-phosphate dehydrogenase) was used as the loading control. Lane 1 : dimethyl sulfoxide (DMSO, vehicle), lane 2 : **2** without light illumination, lane 3 : **2** under 405 nm light illumination (25 mW/cm^2, 10 sec, every 5 min), lane 4 : **2** under 525 nm light illumination (50 mW/cm^2, 10 sec, every 5 min), and lane 5 : **1** (100 μM). MLC-2, myosin light chain II; phospho MLC-2, phosphorylated MLC-2.

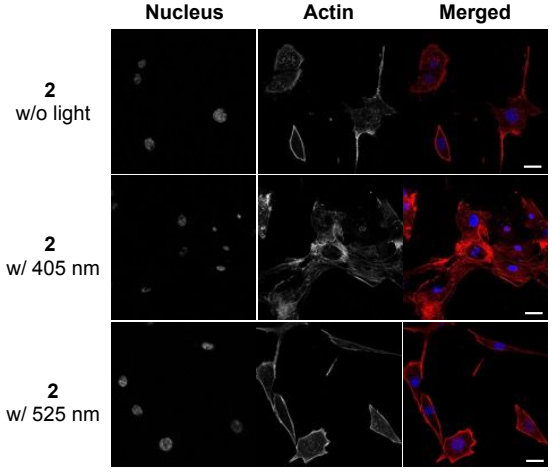

Figure 5. Fluorescence imaging of actin stress fibers in the presence of **2** with or without light stimuli. Cell nuclei were stained with 4′,6-diamidino-2-phenylindole (DAPI). Actin stress fibers were stained with rhodamine-phalloidin. Scale bar : 25 μm. w/, with; w/o, without.

To summarize, we developed a phenylazothiazole derivative **2** as the first photochromic ROCK inhibitor which could reversibly control ROCK activity using visible light illumination at two different wavelengths (405 nm and 525 nm) through the rational design based on the reported x-ray structure. Our results in test tubes and in cells clearly show the photoswitching function of **2** toward ROCK activity through ATPase assays and Western blot analysis, respectively. Our photochemical tool **2** provides the powerful manipulation technique of ROCK-dependent organization of actin stress fibers in the serum starved cells in a photoswitchable manner. However, one drawback of our ROCK inhibitor **2** is a relatively high concentration needed to regulate ROCK activity. We are currently expanding the structure-activity relationship study of the photoswitchable ROCK inhibitors to increase the affinity and photoswitchability. In the future studies, these principles can contribute to the advances in ROCK-based photopharmacology through the improvement of therapeutic index and ROCK controllability with high spatiotemporal resolution.

In this study, the potent characteristics of the 4-monosubstituted phenylazothiazole photoswitch including high photoswitchability with visible light stimuli and the

tolerable anti-reductant property were also highlighted. The thiazole-based photoswitch can be potentially applicable to the versatile biomolecules,[15] some of which are considered as vital therapeutic targets for cancer therapy.[16] We will elaborately expand the biological targets for arylazothiazole photoswitches in future.

This work was performed under the International Cooperative Research Program of "Dynamic Alliance for Open Innovation Bridging Human, Environment and Materials" in "Network Joint Research Center for Materials and Devices" and the technical support platforms for promoting research "Advanced Bioimaging Support". This work was supported by JSPS KAKENHI Grant numbers JP19K15709 (Grant-in-Aid for Early-Career Scientists), JP20H05432 (Grant-in-Aid for Scientific Research on Innovative Areas, "Molecular Movies"), JP21K19317 (Grant-in-Aid for Challenging Research (Exploratory)), and JP19KK0181 (Fostering Joint International Research B) (to K.M.). We would also like to acknowledge the supports of the Adaptable and Seamless Technology Transfer Program through Target-driven R&D (A-STEP) from the Japan Science and Technology Agency (JST) Grant number JPMJTM20A9 and JPMJTM20J9 (to K.M.). This study was also funded by Noguchi Foundation, The Foundation for The Promotion of Ion Engineering, The Akiyama Life Science Foundation, Suhara Foundation, Japan Foundation for Applied Enzymology, Koyanagi Foundation, Inamori Foundation, Research Foundation for Opto-Science and Technology, The Uehara Memorial Foundation (to K.M.) and TOKYO OHKA Foundation for the Promotion of Science and Technology (to N.T.).

Conflicts of interest

There are no conflicts to declare.

Notes and references

1 (a) K. A. Zewdie, M. A. Ayza, B. A. Tesfaye, D. Z. Wondafrash and D. F. Berhe, *Res. Rep. Urol.,* 2020, **12**, 261. (b) A. V. Schofield and O. Bernard, *Crit. Rev. Biochem. Mol. Biol.,* 2013, **48**, 301. (c) M. A. F. de Godoy and S. Rattan, *Trends Pharmacol. Sci.,* 2011, **32**, 384. (d) M. Amano, M. Nakayama and K. Kaibuchi, *Cytoskeleton,* 2010, **67**, 545.

2 (a) J. Shi, X. Wu, M. Surma, S. Vemula, L. Zhang, Y. Yang, R. Kapur, L. Wei *Cell Death Dis.,* 2013, **4**, e483. (b) S. Hartmann, A. J. Ridley, S. Lutz, *Front Pharmacol.* 2015, **6**, 276.

3 (a) Y. Feng, P. V. LoGrasso, O. Defert and R. Li, *J. Med. Chem.,* 2016, **59**, 2269. (b) J. K. Liao, M. Seto and K. Noma, *J. Cardiovasc. Pharmacol.,* 2007, **50**, 17. (c) T. Asano, I. Ikegaki, S. Satoh, M. Seto and Y. Sasaki, *Cardiovas. Drug Rev.,* 1998, **16**, 76. (d) M. Uehata, T. Ishizaki, H. Sato, T. Ono, T. Kawahara, T. Morishita, H. Tamakawa, K. Yamagami, J. Inui, M. Maekawa and S. Narumiya, *Nature,* 1997, **389**, 990.

4 A. R. Morckel, H. Lusic, L. Farzana, J. A. Yoder, A. Deiters and N. M. Nascone-Yoder, *Development,* 2012, **139**, 437.

5 (a) M. J. Fuchter, *J. Med. Chem.,* 2020, **63**, 11436. (b) K. Hüll, J. Morstein and D. Trauner, *Chem. Rev.,* 2018, **118**, 10710. (c) W. A. Velema, W. Szymanski and B. L. Feringa, *J. Am. Chem. Soc.,* 2014, **136**, 2178. (d) A. A. Beharry and G. A. Woolley, *Chem. Soc. Rev.,* 2011, **40**, 4422. (e) M. Borowiak, W. Nahaboo, M. Reynders, K. Nekolla, P. Jalinot, J. Hasserodt, M. Rehberg, M. Delattre, S. Zahler, A. Vollmar, D. Trauner and O. Thorn-Seshold, *Cell,* 2015, **162**, 403. (f) M. Borowiak, F. Küllmer, F. Gegenfurtner, S. Peil, V. Nasufovic, S. Zahler, O. Thorn-Seshold, D. Trauner and H. D. Arndt, *J. Am. Chem. Soc.,* 2020, **142**, 9240.

6 (a) H. D. M. Bandara and S. C. Burdette, *Chem. Soc. Rev.,* 2012, **41**, 1809. (b) J. D. Harris, M. J. Moran and I. Aprahamian, *Proc. Natl. Acad. Sci. U. S. A.,* 2018, **115**, 9414. (c) W. Szymański, J. M. Beierle, H. A. V. Kistemaker, W. A. Velema and B. L. Feringa, *Chem. Rev.,* 2013, **113**, 6114.

7 (a) N. N. Mafy, K. Matsuo, S. Hiruma, R. Uehara and N. Tamaoki, *J. Am. Chem. Soc.,* 2020, **142**, 1763. (b) K. Matsuo and N. Tamaoki *Org. Biomol. Chem.* 2021,**19**, 979. (c) K. R. S. Kumar, T. Kamei, T. Fukaminato and N. Tamaoki, *ACS Nano,* 2014, **8**, 4157. (d) A. S. Amrutha, K. R. S. Kumar, K. Matsuo and N. Tamaoki, *Org. Biomol. Chem.*, 2016, **14**, 7202. (e) N. Perur, M. Yahara, T. Kamei and N. Tamaoki, *Chem. Commun.*, 2013, **49**, 9935. (f) H. M. Menezes, M. J. Islam, M. Takahashi and N. Tamaoki, *Org. Biomol. Chem.*, 2017, **15**, 8894. (g) M. J. Islam, K. Matsuo, H. M. Menezes, M. Takahashi, H. Nakagawa, A. Kakugo, K. Sada and N. Tamaoki, *Org. Biomol. Chem.,* 2019, **17**, 53.

8 (a) R. Siewertsen, H. Neumann, B. Buchheim-Stehn, R. Herges, C. Näther, F. Renth and F. Temps, *J. Am. Chem. Soc.,* 2009, **131**, 15594. (b) A. A. Beharry, O. Sadovski and G. A. Woolley, *J. Am. Chem. Soc.,* 2011, **133**, 19684. (c) Y. Yang, R. P. Hughes and I. Aprahamian, *J. Am. Chem. Soc.,* 2012, **134**, 15221. (d) S. Fredrich, R. Göstl, M. Herder, L. Grubert and S. Hecht, *Angew. Chem. Int. Ed.,* 2016, **55**, 1208.

9 (a) R. Ferreira, J. R. Nilsson, C. Solano, J. Andréasson and M. Grøtli, *Sci. Rep.,* 2015, **5**, 9769. (b) C. L. Fleming, M. Grøtli and J. Andréasson, *ChemPhotoChem,* 2019, **3**, 318. (c) M. Schehr, C. Ianes, J. Weisner, L. Heintze, M. P. Müller, C. Pichlo, J. Charl, E. Brunstein, J. Ewert, M. Lehr, U. Baumann, D. Rauh, U. Knippschild, C. Peifer and R. Herges, *Photochem. Photobiol. Sci.,* 2019, **18**, 1398. (d) M. W. H. Hoorens, M. E. Ourailidou, T. Rodat, P. E. van der Wouden, P. Kobauri, M. Kriegs, C. Peifer, B. L. Feringa, F. J. Dekker, W. Szymanski, *Eur. J. Med. Chem.,* 2019, **179**, 133. (e) L. Heintze, D. Schmidt, T. Rodat, L. Heintze, D. Schmidt, T. Rodat, L. Witt, J. Ewert, M. Kriegs, R. Herges and C. Peifer, *Int. J. Mol. Sci.,* 2020, **21**, 8961.(f) D. Kolarski, C. Miró-Vinyals, A. Sugiyama, A. Srivastava, D. Ono, Y. Nagai, M. Iida, K. Itami, F. Tama, W. Szymanski, T. Hirota, B. L. Feringa, *Nat. Commun.* 2021, **12**, 3164. (g) M. Reynders, A. Chaikuad, B. T. Berger, K. Bauer, P. Koch, S. Laufer, S. Knapp, D. Trauner, *Angew. Chem. Int. Ed.*, 2021, **60**, 20178. (h) Y. Xu, C. Gao, L. Håversen, T. Lundbäck, J. Andréasson, M. Grøtli, *Chem. Commun.* 2021, **57**, 10043.

10 J. Green, J. Cao, U. K. Bandarage, H. Gao, J. Court, C. Marhefka, M. Jacobs, P. Taslimi, D. Newsome, T. Nakayama, S. Shah and S. Rodems, *J. Med. Chem.,* 2015, **58**, 5028.

11 (a) M. Schoenberger, A. Damijonaitis, Z. Zhang, D. Nagel, D. Trauner, *ACS Chem. Neurosci.*, 2014, **5**, 514. (b) J. Broichhagen, J. A. Frank, D. Trauner, *Acc. Chem. Res.*, 2015, **48**, 1947.

12 C. Knie, M. Utecht, F. Zhao, H. Kulla, S. Kovalenko, A. M. Brouwer, P. Saalfrank, S. Hecht, D. Bléger, *Chem. Eur. J.,* 2014, **20**, 16492.

13 A. A. Hassan, N. K. Mohamed, A. A. Aly, H. N. Tawfeek, S. Bräse and M. Nieger, J. Mol. Struct., 2019, 1176, 346.

14 J. C. Yarrow, G. Totsukawa, G. T. Charras and T. J. Mitchison, *Chem. Biol.,* 2005, **12**, 385.

15 A. Ayati, S. Emami, A. Asadipour, A. Shafiee and A. Foroumadi, *Eur. J. Med. Chem.*, 2015, **97**, 699.

16 P. C. Sharma, K. K. Bansal, A. Sharma, D. Sharma and A. Deep, *Eur. J. Med. Chem.*, 2020, **188**, 112016.